Dynamic Thermal Modeling of a Hydronic Heating System

CARMELA CONCILIO, SALVATORE OLIVA, AND GENNARO CUCCURULLO
Dipartimento di Ingegneria Industriale,
Università degli Studi di Salerno,
Via Giovanni Paolo II, 123,
Fisciano (SA),
ITALY

Abstract: - A refined thermal model is presented to describe both the early-stage behavior and the dynamic temperature response of cast iron radiators during heating system operation. In the initial phase, the radiator is conceptually subdivided into three thermally distinct subdomains: the region progressively filled with hot water due to fluid motion, the cast iron wall, and a complementary zone where the fluid remains at its initial (ambient) temperature. Once the radiator is filled with hot fluid, this early stage concludes; however, a downstream adiabatic "short volume" is introduced to account for the delay observed in the outlet temperature rise associated with the fluid transit time through the radiator. The proposed modeling framework offers a physically sound and computationally efficient strategy to simulate both start-up transients and the longer-term dynamic thermal response of radiator-based heating systems.

Key-Words: - Hydronic heating system, dynamic thermal modeling, cast iron radiators, residence time, building energy simulation, radiator thermal inertia, outlet temperature delay, heating system efficiency.

Received: March 16, 2025. Revised: June 2, 2025. Accepted: August 5, 2025. Published: September 30, 2025.

1 Introduction

When a solid body exhibits a Biot number (Bi) significantly smaller than one ($Bi \ll 1$), it is generally expected, excluding very short initial times when boundary condition discontinuities dominate, that the internal temperature distribution remains nearly uniform. This allows a substantial simplification of the heat transfer problem through the use of a lumped-parameter model, where the entire body is treated as a single thermal node, [1], [2]. Such simplification is also justified, although for different reasons, even when the Biot number is large. In fact, at sufficiently long times, any thermal transient tends to decay, and the system approaches a thermal equilibrium with its surroundings. This leads, inevitably, to a flattening of the temperature gradient within the body, as both the internal and boundary temperatures converge. Hence, both in the case of $Bi \ll 1$ (for intermediate-to-long times) and $Bi \gg 1$ (for long times), the lumped formulation provides a valid and physically consistent approximation, greatly reducing the complexity of the model while retaining its descriptive power in typical heating scenarios.

Conversely, when dealing with very small time scales, even in systems characterized by low Biot numbers, significant internal temperature gradients may arise due to the inertia of the material and the rapid imposition of boundary conditions. In this early transient regime, the lumped-capacitance assumption may no longer hold, and a more detailed spatial resolution of the temperature field becomes necessary to accurately capture the initial thermal response. This limitation is particularly relevant when evaluating fast switching phenomena, such as short boiler activations or abrupt environmental changes, where the assumption of internal thermal uniformity would lead to an underestimation of thermal lag and stored energy. Therefore, while the lumped approach offers an efficient and often sufficient representation for most practical scenarios, its applicability must be carefully assessed against the characteristic time and spatial scales of the specific thermal process under investigation.

This is precisely the case of domestic heating radiators, which have long served as terminal units in residential buildings across Europe. These devices provide heat to indoor spaces through a combination of radiation and natural convection. Notably, the capacitive behavior of radiators is currently neglected in most commercially available dynamic simulation tools. Despite their widespread adoption, conventional Building Performance Simulation (BPS) tools—such as EnergyPlus and TRNSYS—have traditionally modelled radiators

using steady-state assumptions only, [3], [4]. However, in certain situations—particularly when heavy cast-iron radiators are used—the heat output can vary considerably during the warm-up and cool-down phases, due to the substantial thermal inertia of these units, which are capable of storing significant amounts of thermal energy. It has been widely demonstrated that radiator models differing in thermal inertia—despite having identical nominal performance—can lead to significant variations in heating loads, indoor temperature profiles, and overall heat pump efficiency, [4], [5], [6], [7].

In this context, this study aims to provide a comprehensive analysis of the heat transfer phenomena occurring in (cast iron) radiators during thermal transients. An easy-to-handle mathematical model is proposed, tailored for use in energy systems analysis, to recover a simplified yet accurate representation of their transient thermal behavior and overall efficiency. To this purpose, a spatially resolved approach is adopted, whereby the radiator domain is divided into thermally distinct subregions. Two characteristic time scales are identified: the first is governed by heat diffusion across the cast iron wall, while the second is associated with the fluid transit time through the radiator. From a dynamic perspective, the latter introduces a delay in the outlet temperature response relative to the inlet conditions.

2 The Early Transient Stage of a Domestic Radiator

The focus of this paragraph is on the initial heating phase of the radiator, during which it is progressively filled with hot water supplied by the boiler, while the complementary region remains at the initial ambient temperature. The progressive thermal activation of the radiator is not instantaneous, but rather governed by the fluid front advancing through the internal channels. In view of the above, the short-time thermal behavior of a domestic heating radiator can be effectively captured by introducing a refined model that decomposes the lumped thermal node into three distinct subcomponents. This three-body representation reflects the non-instantaneous thermal response associated with the transient filling phase, during which the radiator cannot yet be treated as a uniformly heated object. It allows a more accurate description of the initial energy storage process and delays the onset of convective heat transfer to the room until a meaningful surface temperature level has developed.

2.1 The Mass-based Residence Time

The transient filling phase is considered complete once a characteristic time has elapsed. In the thermal modeling of hydronic radiators, two characteristic times are frequently employed, each reflecting a different physical interpretation of the fluid transit process.

The first one is based on the total water mass contained in a single radiator element divided by the corresponding mass flow rate; the residence time is then defined as:

$$t_{\mathrm{res}} = \frac{m_{\mathrm{el}}}{\dot{m}_{\mathrm{el}}} \tag{1}$$

It represents the time required for the entire mass of water contained in the radiator element to be replaced by the incoming hot fluid. This definition accounts for the total volume of fluid in the system and is used to estimate the global thermal inertia and integral transport delay.

The second characteristic time is defined as the axial length of the radiator column, L_{col}, divided by the average flow velocity in the pipe; it represents the time required for a single fluid particle to travel along the longitudinal axis of the radiator, assuming a known average flow velocity v_{col}:

$$t_{\mathrm{kin}} = \frac{L_{\mathrm{col}}}{v_{\mathrm{col}}} \tag{2}$$

These two timescales are not necessarily equivalent, as the velocity-based approach accounts for the effective displacement of the fluid front, whereas the mass-based approach integrates the cumulative water volume required to fill the element. These two definitions yield similar results only under idealized assumptions, such as a uniform velocity field, constant cross-sectional area, negligible stagnant zones, and structural inhomogeneities.

In practice, especially for cast iron radiators, internal geometry is complex, and the actual flow paths are affected by variable cross-sections, non-uniform flow distribution, and dead zones. In the present work, the residence time t_{res} is adopted as the characteristic time associated with the transient propagation of hot fluid inside the radiator. This definition appears to be consistent with a control-volume approach, in which the time required to completely replace the initially cold fluid with hot water reflects the duration of the initial transient phase. Compared to a purely kinematic estimate based on axial length and flow velocity, the mass-based definition ensures compatibility with the thermal capacity of the fluid domain and enables a

consistent treatment of energy accumulation during the warm-up process.

For times shorter than the residence time, the average temperature of the radiator is modeled by dividing the radiator volume into thermally distinct subregions:

1. the hot portion, already filled with hot fluid;
2. the cold portion, still undisturbed at its initial temperature.

The first subcomponent represents the portion of the radiator that is progressively filled with hot water coming from the boiler. This region is assumed to be at a uniform temperature, equal to the inlet water temperature. This assumption is supported by the evaluation of the Péclet number, which quantifies the dominance of longitudinal advection over transverse thermal conduction within the fluid core, see the next paragraph.

The second subcomponent corresponds to the cast iron wall. Given its small thickness, the associated Biot number is well below 0.1, which justifies the use of a lumped-parameter approach to describe its thermal response. Heat exchange is assumed to occur only on the side facing the water flow, due to the significantly larger temperature difference ($\Delta T \approx 70°C - 20°C$) and the higher convective heat transfer coefficient compared to the air side.

The third subcomponent corresponds to the remaining volume of the radiator, complementary to the hot water-filled region and progressively shrinking over time, which retains the initial system temperature—typically equal to the ambient room temperature—before the activation of the heating system.

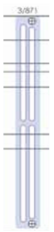

Code 033871	Product Tema 3/871	Height [mm] 875	Center dist. [mm] 813	Depth [mm] 94
Pitch [mm] 60	Water Cont. [lt] 1,00	Weight [kg] 7,7	Emissions Δt=50°C [W] 109,2	Exp 1,289

Fig. 1: Features of a typical cast iron radiator (mod. 3/871)
Source: created by the authors

To support this modeling choice, a set of key dimensionless and dimensional parameters is here evaluated for a typical radiator element. A typical three-column cast iron radiator element, catalogued by Ideal Clima srl, Brescia, Italy, is considered, as shown in Figure 1. Excluding the top and bottom manifolds, the effective vertical flow length is assumed to be equal to 800 mm. Each column is approximated as a vertical cylinder of 30 mm diameter.

2.2 About the Uniform Inlet Temperature in the Hot Region

Under nominal operating conditions, each element delivers 109.2 W of thermal power. Therefore, the nominal mass flow rate per element (subscript "el") is:

$$\dot{m}^*_{\mathrm{el}} = \frac{\dot{q}^*_{\mathrm{el}}}{c_{\mathrm{w}}(T^*_{\mathrm{inlet}} - T^*_{\mathrm{outlet}})} = 0.0026\,\frac{\mathrm{kg}}{\mathrm{s}} \qquad (3)$$

where the superscript "*" refers to the standard design operating conditions ($T^*_{\mathrm{inlet}} = 75°C$; $T^*_{\mathrm{outlet}} = 65°C$; $T^*_{\mathrm{amb}} = 20°C$) and c_{w} is the specific heat of water (4187 J/kg·K). Distributing this equally among the three vertical columns yields the flow rate per column, i.e.

$$\dot{m}^*_{\mathrm{col}} = \frac{\dot{m}^*_{\mathrm{el}}}{3} = 3.13\,\frac{\mathrm{kg}}{\mathrm{h}} \qquad (4)$$

Therefore, the column diameter being D_{col} = 30 mm, the water velocity in a column turns out to be $v_{\mathrm{col}} \approx 1.23$ mm/s. Considering a characteristic transverse length equal to the column diameter and a water thermal diffusivity of α=1.56×10−7m^2, the Péclet number (*Pe*), a measure of the relative magnitude of axial convective flow compared to radial conductive flow, is obtained as *Pe* = 238. This confirms that longitudinal advection largely outweighs axial thermal conduction, justifying the assignment of a uniform inlet temperature to the hot fluid entering the radiator.

2.3 About the Lumped Approach for the Cast Iron Wall

For the internal convective heat transfer, assuming a kinematic viscosity of $\nu = 4.04 \times 10^{-7}$ m²/s and a thermal conductivity of k = 0.665 W/(m·K) for water at 70°C, as well as a hydraulic diameter of D□ = 30 mm, the Reynolds number corresponding to a mass flow rate of 3.13 kg/h is approximately *Re* ≈ 100, which confirms laminar flow conditions. Under the assumption of fully developed flow and constant wall temperature—a conservative scenario in terms of heat transfer—the Nusselt number can be taken as *Nu* = 3.66, [8], leading to the following estimate for the internal convective heat transfer coefficient:

$$Nu = 3.66 \Rightarrow h = Nu\frac{k}{D} \approx 80\frac{\mathrm{W}}{\mathrm{m}^2\ \mathrm{K}} \quad (5)$$

The knowledge of the internal heat transfer coefficient h allows for the calculation of the thermal time constant of the radiator's cast-iron wall. As previously justified, the wall is assumed to be thermally insulated on the air-facing side, with heat exchange occurring exclusively on the side in contact with the internal water flow. The cast iron wall is modeled as a thin slab with a thickness of s_h =4 mm, density ρ_h=7200 kg/m^3, specific heat c_h=500 J/kg/K, thermal conductivity k_h=50 W/m/K. Since only one face of the slab is thermally active, the Biot number is defined as:

$$Bi = h\frac{2s_h}{k_h} = 80\ 2\frac{4\ 10^{-3}}{50} = 0.0128 \quad 0.1 \quad (6)$$

which justifies the use of the lumped-capacitance approximation.

Moreover, since the characteristic diffusion time of the cast iron slab can be estimated as $L^2/\alpha \approx 1$ s, which is much shorter than the timescales of interest in the present problem, the lumped-capacitance assumption is strongly supported.

The above analysis enables the estimation of the thermal time constant $t_{h,}$ of the cast iron wall:

$$t_h = \rho_h\ c_h 2s_h / h = 360\ \mathrm{s} \quad (7)$$

which governs the exponential rise in wall temperature.

2.4 Thermal Performance

The mean surface temperature of the radiator plays a crucial role in determining its overall thermal performance, as it directly governs the combined convective and radiative heat exchange with the surrounding environment. The modeling framework introduced in the previous section provides the necessary basis to evaluate this temperature with accuracy.

During the early transient stage, the portion of the radiator already filled with hot fluid transfers heat to the cast iron wall, whose temperature increases following an exponential law governed by the wall's thermal time constant $t_{c,w}$,

$$\bar{T}_h = T_{inlet} + (T_{amb} - T_{inlet})\ \exp(-t / t_{c,h}) \quad (8)$$

Meanwhile, the cold portion of the radiator remains undisturbed at its initial temperature $\bar{T}_c = T_{amb}$.

To represent the progressive advancement of the hot fluid front, a *filling function* $a(t) = t / t_{res}$ is introduced, where t_{res} is the residence time, as defined in the previous section. This linear function evolves from 0 (completely cold radiator) to 1 (filled radiator).

The mean radiator temperature during the early transient stage, $\bar{T}_{es}$, is then expressed as:

$$\bar{T}_{es} = a(t)\bar{T}_h + \bar{T}_c(1 - a(t)) + b\,t^2 \quad (9)$$

The first two terms represent the weighted contributions of the undisturbed cold portion and the heated portion of the radiator. The third term is a quadratic correction introduced to ensure continuity of the time derivative of the mean radiator temperature at the transition time t = tres; therefore, the coefficient b is computed to satisfy the following condition:

$$\left.\frac{\partial \bar{T}_{es}(t,b)}{\partial t}\right|_{t=t_{res}^-} = \left.\frac{\partial \bar{T}_{ls}(t)}{\partial t}\right|_{t=t_{res}^+} \quad (10)$$

where the function $\bar{T}_{ls}(t)$ denotes the mean temperature in the subsequent stage. This constraint ensures that the rate of change of the thermal energy stored in the radiator evolves smoothly, avoiding artificial jumps when switching from the early to the late stage. Such an approach is consistent with the principles of piecewise dynamical modeling, where continuity of both the state variables and their derivatives is imposed to ensure physically consistent transients, [9], [10], [11].

3 The Late Transient Stage

Once the radiator is filled with hot fluid—marking the end of the early transient stage—the system enters a new regime in which the thermal dynamics are governed by the interaction between the entire cast iron mass and the continuous inflow of hot water. In this late transient stage, the evolution of the radiator's temperature is described by a differential equation derived from a lumped energy balance, which captures both the advective heat input from the fluid and the diffusive thermal losses to the surrounding environment. The energy balance is formulated under the following simplifying assumptions: 1 - constant fluid properties, 2 - negligible gravitational and kinetic effects, 3 - fixed ambient conditions, reflecting standard indoor conditions.

3.1 The Lumped Energy Balance

Under these assumptions, the energy balance applied to the radiator system takes the following form:

$$C_{\text{rad}} \frac{\partial \bar{T}_{\text{ls}}}{\partial t} = e\ \dot{m}^{*}_{\text{el}}\ c_{\text{w}}\ (T_{\text{inlet}} - T_{\text{outlet}}) + \dot{Q}_{\text{diff}} \quad (11)$$

where: e is the radiator element number, C_{rad} is the total thermal capacity of the radiator, including both cast iron and contained water, $\dot{Q}_{\text{diff}}$ and is the heat power released from the radiator to the surrounding room environment.

The above energy balance can be formulated in accordance with the guidelines provided by standards such as [12], [13], [14]. These standards recommend adopting a semi-empirical power-law expression to describe the diffusive heat flux from the radiator surface to the ambient environment:

$$\frac{\dot{Q}_{\text{diff}}}{e\ \dot{q}_{\text{ref}}} = \left(\frac{\bar{T}_{\text{ls}} - T_{\text{amb}}}{\Delta T_{\text{ref}}} \right)^{\text{n}} \quad (12)$$

This formulation accounts for the combined convective and radiative heat transfer, both of which exhibit nonlinear dependence on the surface-to-air temperature difference.

3.2 The Use of the Arithmetic Mean Temperature Difference

Moreover, the aforementioned standards recommend the use of the arithmetic mean temperature difference (AMTD)—rather than the logarithmic mean temperature difference (LMTD)—when calculating the radiator's effective surface temperature. While LMTD is classically employed in the analysis of heat exchangers to account for the spatial variation of the temperature difference between the hot and cold fluids, its application assumes ideal flow configurations and uniform thermal conditions. The relationship between the two averages can be expressed as a function of the dimensionless parameter z, as discussed in [9]:

$$\text{LMTD} = \frac{\Delta T_0 z}{\ln(1+z)} < \frac{\Delta T_{\text{L}} + \Delta T_0}{2} = \text{AMTD} \quad (13)$$

To validate the use of AMTD as a substitute for LMTD, a numerical comparison was carried out using standard radiator design conditions already defined; for these values, the parameter z results in 0.222, and the ratio between LMTD and AMTD evaluates to 0.997. These results confirm that, under typical conditions, the difference between LMTD and AMTD is less than 0.4%. This negligible deviation justifies the use of the arithmetic mean temperature difference as a practical and accurate approximation for modeling the radiator's thermal behavior, in accordance with current standards and building energy simulation practices.

The use of the arithmetic mean enables us to express the energy balance as a function of the unknown outlet temperature:

$$C_{\text{rad}} \frac{1}{2} \frac{\partial T_{\text{outlet}}}{\partial t} = e\ \dot{m}^{*}_{\text{el}}\ c_{\text{w}}\ (T_{\text{inlet}} - T_{\text{outlet}}) + \\ + e\ \dot{q}_{\text{ref}} \left(\frac{\bar{T}_{\text{ls}} - T_{\text{amb}}}{\Delta T_{\text{ref}}} \right)^{\text{n}} \quad (14)$$

3.3 The Delayed Thermal Response at the Radiator Outlet

In the previous equation, the outlet temperature is treated as a dynamic variable determined by the energy balance applied to the entire radiator body. However, this formulation alone neglects the convective transport delay inherently associated with the finite residence time of the fluid as it flows through the radiator's internal channels. To account for this non-instantaneous thermal response, a second differential equation is introduced. This models a small adiabatic control volume placed at the outlet, which—despite being thermally insulated—retains a limited thermal inertia that introduces a delay between the average radiator temperature and the actual temperature of the exiting fluid. This modelling approach is consistent with the methodology proposed in [10], who demonstrated that transport delays in heat exchangers can be effectively captured through time-delay differential formulations. In this context, the lumped outlet node combined with a residence-time parameter provides a compact yet physically meaningful representation of the delayed outlet response. This delayed thermal response is modelled through a first-order lumped dynamic system, which ensures correct time alignment with the residence time by introducing a delayed outlet effect consistent with the flow path through the radiator:

$$\frac{\partial T^{\text{delayed}}_{\text{outlet}}(t)}{\partial t} = \frac{T_{\text{outlet}}(t) - T^{\text{delayed}}_{\text{outlet}}(t)}{t_{\text{res}}} \quad (15)$$

The small-volume model introduced at the radiator outlet represents a compromise between two competing needs. On the one hand, it reflects physical realism, acknowledging that the fluid does not instantaneously adopt the mean radiator temperature, but requires a finite residence time for

heat to be transported by convection. On the other hand, it preserves modelling simplicity, avoiding the complexity of solving the full one-dimensional energy equation. The effect is reproduced by a single additional lumped node, thermally adiabatic but dynamically responsive, which captures the essential delay with minimal complexity. This formulation can therefore be interpreted as a compact representation of transport delay, consistent with the method of characteristics and with time-delay approximations commonly used in heat exchanger modelling [10]. In this framework, lumped dynamic nodes are a standard tool to capture convective transport delays while preserving both computational efficiency and physical interpretability.

4 Results and Discussion

The following numerical results are presented with reference to the previously identified commercially available radiator model. The inlet operating conditions are fixed at their nominal design values: an inlet water temperature of 75 °C and a constant mass flow rate of 9.38 kg/h, the latter corresponding to a residence time of t_{res} = 383 s.

The solution describing the early-time behavior is then coupled with the one valid for the late-time dynamics. A smooth transition between the two regimes is achieved by enforcing continuity in both the average radiator temperature and its time derivative at the switching point t=t_{res}. The resulting coupling condition, exposed in equation (10), can be explicitly formulated in terms of the coefficient b, which characterizes the quadratic approximation adopted for the early-time temperature profile:

$$\left.\frac{C_{rad}}{e}\frac{\partial \bar{T}_{es}(t,b)}{\partial t}\right|_{t=t_{res}^{-}} = \dot{m}_{el}^{*}\, c_w\, 2(T_{inlet}-\bar{T}_{es}(t_{res},b)) + \\ +\dot{q}_{ref}\left(\frac{\bar{T}_{es}(t_{res},b)-T_{amb}}{\Delta T_{ref}}\right)^{n} \quad (16)$$

This yields the value $b = -4.81\times10^{-5}$ °C/s^2.

Then, the two coupled differential equations, eq. (11) and (15) are solved with the following initial conditions imposed at the beginning of the late-time period:

$$\begin{cases} T_{outlet}(t_{res}) = 2\bar{T}_{es}(t_{res},b) - T_{inlet} \\ T_{outlet}^{delayed}(t_{res}) = T_{amb} \end{cases} \quad (17)$$

Both equations are numerically integrated using an explicit fourth-order Runge–Kutta method with adaptive step-size control, ensuring accuracy and numerical stability over the entire simulation time window.

Knowledge of the outlet temperature T_{outlet} enables the computation of the thermal power delivered to the ambient. The second state variable, i.e., the delayed outlet temperature, is relevant for defining proper control logics for the heat generator in future developments.

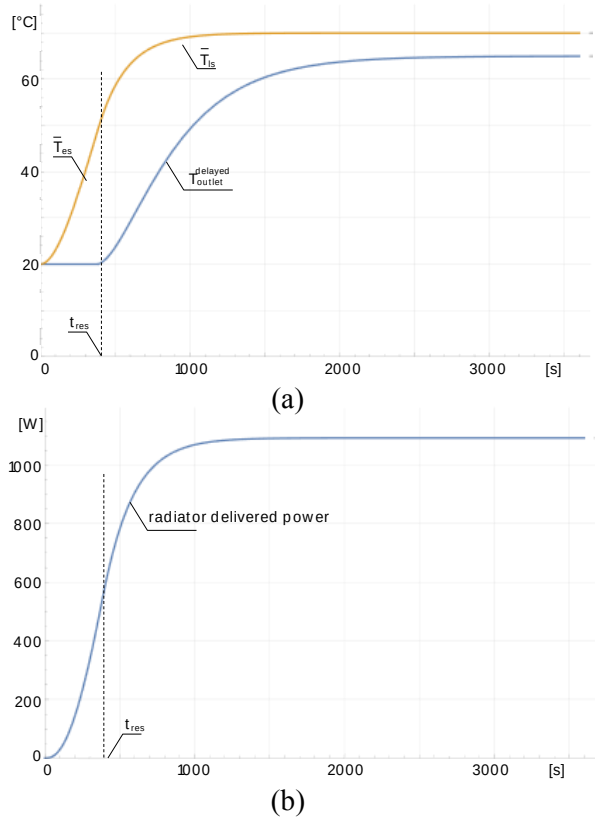

Fig. 2: Time evolution of the state variables
Source: created by the authors

Figure 2(a) shows the time evolution of the state variables. The average radiator temperature during the early stage rises gradually from the initial ambient temperature, with a zero initial slope, as expected due to the imposed smooth quadratic approximation. This initial behavior reflects the progressive increase of the thermal exchange surface within the radiator, where only a small portion near the inlet becomes active in the first instants. As time advances, the heating front advances through the radiator body, resulting in a more rapid increase in the delivered heating power.

The delayed outlet temperature remains fixed at the ambient value throughout the residence time, effectively capturing the delay introduced by convective transport. This result confirms that, until

the fluid has physically traversed the radiator, the outlet temperature cannot carry information about the internal thermal dynamics. It starts to increase only once the heated fluid reaches the outlet, thereby showing a delayed thermal response relative to the average radiator temperature.

Both temperature curves show smooth, monotonic increases and converge asymptotically toward their steady-state values. This behavior ensures consistency with the physical expectations for a thermally driven system subject to a step change in inlet conditions. The correct asymptotic limits further validate the modeling approach and the matching conditions at $t = t_{res}$.

Figure 2(b) reports the evolution of the heating power delivered to the ambient. The curve starts from zero with zero initial slope, as a direct consequence of the smooth rise in the average radiator temperature and in accordance with the physical constraint that no heat is exchanged under initial thermal equilibrium conditions. As the average temperature increases, the delivered power follows a smooth, convex trajectory, gradually steepening as the temperature difference between the radiator and the environment grows. An inflection point can be observed in the power curve, indicating the transition from the early-time regime, governed by the gradual thermal buildup, to the late-time regime, in which the radiator approaches steady-state operation. Eventually, the power output stabilizes at a value close to the nominal design specification, which corresponds to the steady-state thermal load assumed in the design.

The observed results suggest that the proposed model is capable of accurately reproducing the essential qualitative and quantitative characteristics of the transient thermal response—namely, the effects of thermal inertia, the delayed outlet behavior, and the time-dependent evolution of the delivered power, all consistent with the underlying physical principles.

5 Conclusion

A compact and physically grounded dynamic model for a hydronic radiator has been proposed, with specific attention to capturing both early and late-stage thermal behaviours. In the early phase, the approach is not merely aimed at reproducing the initial transients, but at enabling a spatial decomposition of the radiator domain into zones characterized by different thermal conditions. This includes the progressive engagement of the radiator's length as the fluid advances and exchanges heat with the surrounding environment.

For later times, a lumped-capacitance formulation is employed, integrated with a delayed outlet node that accounts for the finite residence time of the fluid. This hybrid formulation captures the essential dynamics of the system with minimal computational complexity. The smooth transition between stages is ensured by enforcing continuity in both temperature and its time derivative at the switching point.

The model structure is particularly suitable for applications requiring simplified but thermally realistic representations, such as building energy simulations or control design. In particular, the delayed outlet temperature serves as a potential input for regulation strategies based on return temperature and anti-cycling logic. The same modelling philosophy is extendable to other components—such as distribution piping—allowing for generalized characterizations of thermal inertia throughout the system.

Future work will focus on coupling the entire thermal plant model with the ambient environment and its boundary walls, treated as one-dimensional distributed objects. This will allow for a more comprehensive assessment of the model's capability to reproduce realistic operating conditions and to support the design of effective thermal regulation strategies.

References:

[1] Incropera, F. P., DeWitt, D. P., Bergman, T. L., Lavine, A. S., *Fundamentals of Heat and Mass Transfer*, 6th ed., Wiley, Hoboken, NJ, USA, 2007.

[2] Çengel, Y. A., Ghajar, A. J., *Heat and Mass Transfer: Fundamentals and Applications*, 5th ed., McGraw-Hill, New York, NY, USA, 2015.

[3] Holst, S., "TRNSYS-Models for Radiator Heating Systems. Types 361, 362 and 320," 1996.

[4] Calise, F., Cappiello, F., Cimmino, L., Dentice, M., Vicidomini, M., "A Novel Capacitive Model of Radiators for Building Dynamic Simulations," *Thermo*, Vol. 5, No. 1, pp. 9–24, 2025.

[5] Belmonte, J. F., Almendros-Ibáñez, J. A., "Integration of dynamic radiator models in building performance simulation tools. Effects of radiator thermal capacitance on buildings' heating system efficiency," in *Proc. Building Simulation 2023: 18th Conf. of IBPSA*, Shanghai, China, Sep. 2023, Vol. 18, pp. 3042–3049.

[6] Zhang, L., Tan, H., "A dynamic model of radiator heating systems for building thermal simulations," *Energy and Buildings*, Vol. 87, pp. 1–11, Jan. 2015.

[7] Xu, B., Fu, L., Di, H., "Dynamic simulation of space heating systems with radiators controlled by TRVs in buildings," *Energy and Buildings*, Vol. 40, No. 9, pp. 1755–1764, 2008.

[8] Bejan, A., *Convection Heat Transfer*, 4th ed., Wiley, Hoboken, NJ, USA, 2013.

[9] *(text in Italian)* Cuccurullo, G., *Termodinamica e trasmissione del calore – Fondamenti e applicazioni*, Maggioli Editore, 2020.

[10] Hamze, S., Witrant, E., Bresch-Pietri, D., Fauvel, C., "Estimating heat transport and time delays in a heat exchanger," in *Proc. 2nd IEEE Conf. Control Technol. Appl. (CCTA)*, Copenhagen, Denmark, Aug. 2018, pp. 1514–1519.

[11] Oppenheim, A. V., Willsky, A. S., *Signals and Systems*, 2nd ed., Prentice Hall, Upper Saddle River, NJ, USA, 1997.

[12] UNI EN 832:1999, *Thermal performance of buildings — Calculation of energy use for heating — Residential buildings*, UNI, 1999.

[13] *(text in Italian)* UNI/TS 11300-2:2019, *Prestazioni energetiche degli edifici – Parte 2: Determinazione del fabbisogno di energia primaria e dei rendimenti per la climatizzazione invernale e l'acqua calda sanitaria*, UNI, 2019.

[14] EN ISO 15316-2:2017, *Energy performance of buildings – Method for calculation of system energy requirements and system efficiencies – Part 2: Space emission systems (heating systems in buildings)*, ISO, 2017.

Contribution of Individual Authors to the Creation of a Scientific Article (Ghostwriting Policy)

The authors equally contributed to the present research, at all stages from the formulation of the problem to the final findings and solution.

Sources of Funding for Research Presented in a Scientific Article or Scientific Article Itself

No funding was received for conducting this study.

Conflict of Interest

The authors have no conflicts of interest to declare that are relevant to the content of this article.